# Methanol assisted water electrooxidation on noble metal free perovskite: RRDE insight into the catalyst's behaviour

*Shikha Dhakar*[†], *Sanchayita Mukhopadhyay*[‡], *Musthafa Ottakam Thotiyl*[‡], *Sudhanshu Sharma*[†]*

[†]*Department of Chemistry, Indian Institute of Technology Gandhinagar, Gandhinagar – 382355*

[‡]*Department of Chemistry, Indian Institute of Science Education and Research, Pune, Maharashtra 411008, India*

[*] Email: ssharma@iitgn.ac.in; (079)23952439, orcid.org/0000-0002-5217-9941

**Corresponding author - Email: ssharma@iitgn.ac.in*

## ABSTRACT:

In this work we have hypothesized that noble metal-free perovskites are an essential class of oxygen evolution reaction (OER) catalysts in an alkaline medium and thus they are a suitable candidate for the assisted water oxidation catalysts. Herein, we demonstrate that the origin of the methanol assisted OER activity at near thermodynamic potential on perovskite electrode arises due to the involvement of additional hydroxyls as a result of dissociative chemisorption of methanol. When the perovskite electrode is screened for methanol electrooxidation reaction in 0.5 M KOH + 0.5 M methanol electrolyte, it delivers a two times higher current density. This imparts an 82% increase in the evolution of oxygen gas moles with complete oxidation of methanol to carbon dioxide. Along with the electrochemical characterization to understand the electrocatalyst property, RRDE technique is explored for the first time in literature to validate the catalyst's involvement during OER. RRDE is found effective to understand the lattice oxygen behaviour and methanol assisted electrooxidation of water during OER. Our results suggest new insights and ideas towards oxygen evolution reaction process and the mechanistic insight into the elevated OER due to assisted methanol electrooxidation.

**Keywords:** Perovskite, electrochemical oxidation, oxygen evolution reaction, lattice oxygen

## 1. INTRODUCTION

The environment is getting polluted due to the release of greenhouse gases from various sources, including industries and automobile engines[1]. Heavy vehicles that consume fossil fuels are one of the significant sources of the emission of toxic gases like CO, $CO_2$, $SO_2$, and NO. In this context, greener fuels that can stave off climate change include biofuels, biogas, and hydrogen produced from water splitting[2].

Incessant efforts have been made to the water-splitting field during the past few years[3] as it is a prospective solution for energy and environment-related problems[2] and their large-scale practical applications in the near future. Electrocatalytic water splitting is a viable and scalable energy technology for the utilisation of renewable energies. It consists of two half-reactions, anodic oxygen evolution reaction (OER) and cathodic hydrogen evolution reaction (HER). OER involves sluggish kinetics[4], which takes place at a theoretical potential of 1.23 V under standard conditions. OER has a high activation energy barrier for O-O bond formation that is a significant bottleneck in the efficiency of many energies' storage technologies[5], like rechargeable metal-air batteries and hydrogen production from electrocatalytic water splitting reaction.

The problem of efficiency of the water splitting reaction can be solved by tuning anodic water oxidation with the simultaneous oxidation of other more readily oxidizable species like alcohol[6,7]. Owing to the good electrochemical activity, availability, and biodegradability of $CH_3OH$ and $C_2H_5OH$, both are beneficial as an alternative source of energy[8]. Methanol is an economical and readily available raw material, initially proposed by Professor George A. Olah for fuel cell applications[9]. Different electrode materials based on Pt[10,11], Pd[12] and Pt-binary electrodes[13] were commonly used as catalysts to accelerate the activity and to overcome the sluggish kinetics and high overpotential for the electrochemical oxidation of methanol. To

overcome such problems, alternative economic transition metals like Ni, Rh, Au and metal oxides such as NiO[14], $Co_3O_4$[15], $CeO_2$ decorated nano ZSM-5 catalyst[16] and complex ternary oxides such as perovskite[4] are being tested for the electrocatalytic oxidation of methanol. Perovskites are probably the most studied mixed-oxide system and are considered a substitute for noble metals in heterogeneous catalysis[17,18]. Gustav Rose in 1839 reported perovskite, which Russian mineralogist L.A. Perovski[19] later gave the name perovskite. Doping the A site with an alkaline earth metal will result in additional oxygen vacancies being generated, which will increase the catalytic activity of ABO3 perovskite oxides[20,21]. Significant literature is available for $La_{0.8}Sr_{0.2}CoO_3$ perovskite as an efficient and stable OER electrocatalyst[22,23]. Nevertheless, its use in methanol electrooxidation has not been explored much. It is well known that the methanol electrooxidation as well as OER happens using adsorbed hydroxyls over the catalyst's surface in a basic electrolyte medium[24–26]. Thus, considering hydroxyls as the common intermediate, both the reaction can occur in assistance with each other. Methanol has been shown to assist OER on several different catalysts reported in the literature[27,28].

In this regard, the electrochemical performance of the noble metal free $La_{0.8}Sr_{0.2}CoO_3$ perovskite is investigated for the possibility of electrooxidizing water at or near the thermodynamic potential in assistance with $CH_3OH$ electrooxidation. In short, it is explored if the catalyst, $La_{0.8}Sr_{0.2}CoO_3$ can reduce the OER overvoltage while oxidising the methanol in parallel. Rotating ring disk electrode (RRDE) is used to validate this phenomenon which in addition imparts very interesting and accurate information related to lattice oxygen participation during the electro oxidation.

***LSCO: A Reservoir of Lattice Oxygen Validation by RRDE***

The lattice oxygen evolution reaction (LOER) must be taken into consideration in order to completely comprehend the mechanism of the water splitting reaction[18,29]. The idea of an alternate approach to the traditional proton-coupled electron transfer (PCET), wherein molecular oxygen is created via the participation of metal oxide and/or perovskite lattice oxygen, was proposed in a few research about OER catalysts in the early 1970s to the 1980s. However, only in the last few years a more rigorous assessment of the lattice oxygen participation has been provided by different research groups[22,30–35]. Recently, Hardin and co-workers investigated the participation of lattice hydroxide species in forming surface-adsorbed hydroperoxides for OER on $LaNiO_3$, $LaMnO_3$, and $LaCoO_3$ catalyst[36]. Generally, the participation of lattice oxygen on LSCO compound has been validated by $H_2$ – TPR studies[37], XPS studies[33,38–40] and isotope labelling together with the differential electrochemical mass spectrometry (DEMS) method[41]. In a completely new approach, we are reporting RRDE to validate this phenomenon. Mostly, RRDE technique is used to calculate the number of electrons transferred in the oxygen reduction reaction (ORR). However, this technique is explored for the first time in literature to understand the involvement of LSCO's lattice oxygen in OER and methanol assisted OER. Experimental data clearly proves that RRDE accurately monitors the lattice oxygen participation in the perovskite. Although, its explicit effect on catalysis is not obvious.

## 2. MATERIALS AND METHODS

### 2.1 Synthesis

$La_{0.8}Sr_{0.2}CoO_3$ catalysts were synthesized through a solution-combustion (self-propagating high-temperature synthesis) process. In brief, stoichiometric quantities of commercial $La(NO_3)_3.6H_2O$ (Aldrich, 99.9%), $Sr(NO_3)_2$ (Aldrich, 99%), and $Co(NO_3)_2{\cdot}6H_2O$ (Aldrich, 99%) precursors as an oxidizing agent were prepared in hot Millipore water (saturated aqueous solution of metal nitrate), and added to solution of ODH. The solution was then heated under

stirring to get the homogeneous transparent solution. The reaction proceeds rapidly following ignition. The transparent solution was ignited to flame in a muffle furnace preheated at 450 °C to start an exothermic reaction that would maintain a high temperature long enough to decompose ODH and metal nitrate salts. The resulting product is in the form of a dry powder. The powder was crushed adequately and calcined for 12 h at 800°C in the air with a 5°C /min rate to get the final black compound.

### 2.2 Material Characterization

The morphology of the synthesized electrocatalyst was analyzed by a JEOL (JSM-7900F) scanning electron microscope (SEM) at high and low magnification. An energy-dispersive X-ray spectrometer (EDS) instrument attached to the SEM, with AZtec (Oxford Instruments) software, was used to determine the composition of the catalyst. The catalyst was mounted onto an aluminium block using double-sided carbon tape. Then, it was coated with gold for 60 seconds to ensure better surface visibility and prevent the sample's electrical charging during analysis. X-ray diffraction (XRD) technique was used to determine the crystal structure and phase constitution of the Perovskite catalyst. A BRUKER D8 DISCOVER diffractometer was used with a Cu X-ray tube source ($\lambda K\alpha = 1.5406$ Å) for X-ray diffraction (XRD) measurements. The working current and voltage for the XRD were 40 mA and 40 kV, respectively. Continuous scans were carried out at a rate of 4°/min (0.04° step size) from 20° to 90° (2θ mode). PDF-4 (International Centre for Diffraction Data) software was used to identify XRD patterns. Transmission electron microscopy (TEM) images were attained using an FEI, Themis 60-300 with EDS detector and FEI-Ceta 4k*4k camera operated at 200 kV.

### 2.3 Electrochemical measurements

The electrochemical experiments were evaluated using a conventional three-electrode glass cell equipped with Auto lab potentiostat (AUTOLABPGSTAT302 N, Metrohm). The electrodes

were glassy carbon electrode (GCE) polished with alumina powder and modified with LSCO catalyst as a working electrode. Pt-wire was used as an auxiliary electrode and a saturated $Ag/AgCl/Cl^-$ (3.5 M KCl) as a reference electrode. The polished GCE had a surface area of 0.071 $cm^2$ and a diameter of 3 mm. The cyclic voltammograms (CV) and chronoamperometric (CA) traces of the catalysts were investigated in an alkaline electrolyte with and without methanol (MeOH) at different concentration under ambient conditions. For performing the hydrodynamic studies, the rotating ring disk electrode (RRDE) method was used where the electrochemical cell was equipped with a GC-Au (glassy carbon disk and Au ring) as working electrode, a Pt mesh as counter electrode, an $Ag/AgCl/Cl^-$ (3.5 M KCl) as reference electrode and 0.5 M KOH as electrolyte. The GC disk has a geometrical surface area of 0.2472 $cm^2$ whereas the Au ring has a geometrical surface area of 0.1859 $cm^2$. The catalyst slurry was drop casted onto the GC disk electrode. Unless otherwise stated, all the RRDE measurements were done at a rotation of 1600 rpm and the currents were normalized with respect to their geometrical surface area. In all measurements, potential in Ag/AgCl is converted to RHE in 0.5 M KOH according to the following equation:

$$E_{RHE} = E_{Ag/AgCl} + 0.059*pH + 0.1976\ V$$

**2.4 Preparation of the modified electrode**

As a working electrode, a glassy carbon electrode (GCE) with a 3 mm diameter was chosen. The working electrode was produced by mixing 50 mg of catalyst with 50 µL of 5% nafion solution as a binder and 200 µL of isopropanol to generate a thin slurry. This mixture was then sonicated for 30 minutes and then deposited over a 0.071 $cm^2$ region on the glassy carbon (GCE) electrode. The working electrode was cleaned by mechanical polishing with alumina suspension and rinsed with copious amounts of Millipore water. About 3 µL solution of the synthesized catalyst in isopropanol dispersion was drop casted on GCE, and IPA was

evaporated at ambient temperature for electrochemical studies. UHP Nitrogen was sparged to the electrochemical cell prior to each experiment to eliminate the dissolved oxygen.

The electrochemical cell was enclosed with parafilm, silicon rubber septum, and vacuum grease to attain an air-tight condition and ensure no product gas leakage from the cell. The High precision gas-tight syringe was used to transfer the evolved gases from headspace into a gas chromatograph (GC; Dhruva CIC Baroda). A thermal conductivity detector and Flame Ionisation Detector was used to quantify the generated gas during electrocatalysis. The standard gas mixture was used for GC Calibration, and the carrier gas used was argon.

## 3. RESULTS AND DISCUSSION

### 3.1 Structure and morphology characterization

Figure 1(a) shows a detailed powder XRD analysis of the synthesized LSCO electrocatalyst. Intense and sharp peaks confirm the excellent crystallinity of LSCO in XRD pattern. As shown in Figure 1(a), all the diffraction peaks of the compounds can be well identified as rhombohedral crystal structural. The prominent crystalline peaks at $2\theta = 23.1°$, 32.8°, 33.14, 47.4°, 58.8° are attributed to the crystal planes of (012), (110), (104), (024) and (214) with R-3c space group symmetry for the LSCO catalyst. Scherrer's equation was used to calculate the average crystallite size, which was determined to be 28.1 nm (expressions is presented in the supplementary information in section 2.2). The absence of segregated Sr and Co species phases supports the creation of a single-phase compound. $LaSrCoO_3$ may have formed as a Rhombohedral-type structure, comparable to $LaCoO_3$, according to the pattern.

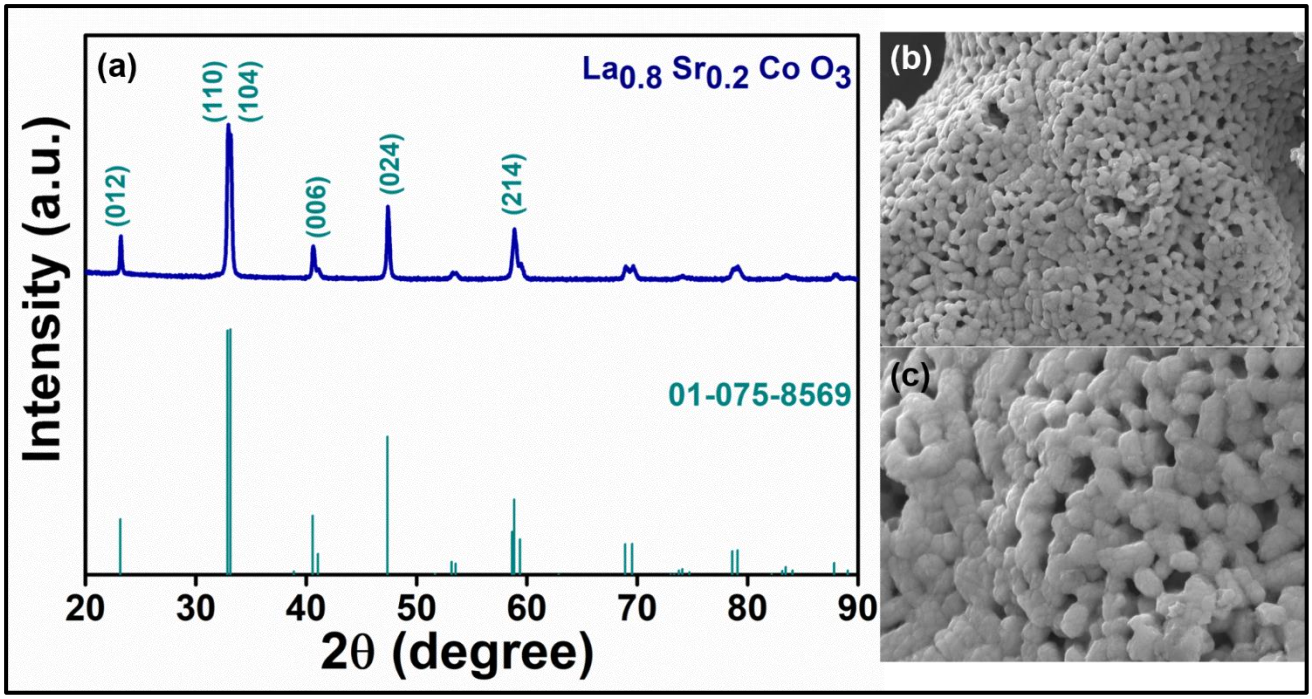


**Figure 1**: *(a) X-ray Diffraction pattern of crystalline LSCO. FESEM image of as synthesized perovskite at magnification of (b) 10,000 and (c) 25,000.*

The substitution of Sr in the $LaCoO_3$ structure has been reported to increase the agglomeration[42]. SEM images are composed of crystalline network-like structures with varying grain sizes. Furthermore, it appears that the grain particles are made up of aggregated spherical particles.

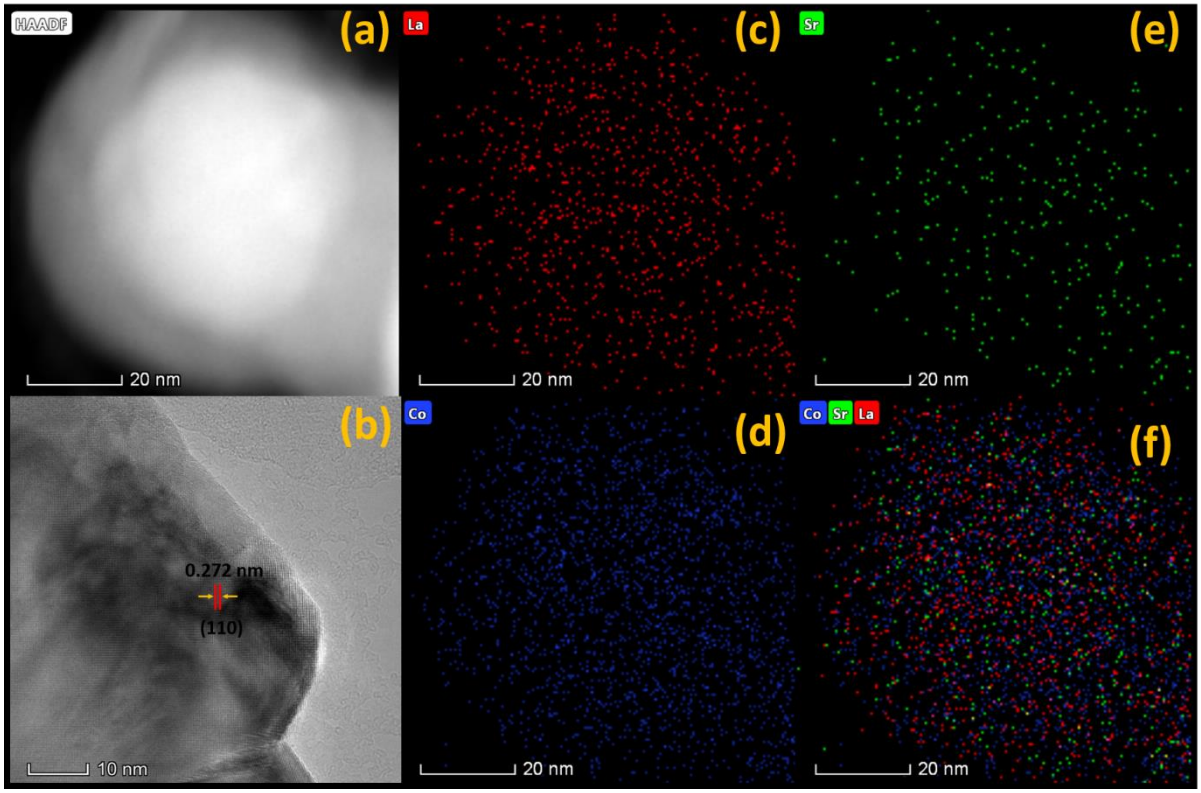


**Figure 2:** *(a) HAADF-STEM image of LSCO, (b) HRTEM image of LSCO at 10 nm magnification indicating d spacing of 0.272 nm, (c-e) elemental mapping for La, Co and Sr respectively, (f) mixed elemental mapping of LSCO.*

To better understand the morphology and crystalline property of LSCO perovskite, high-resolution transmission electron microscopy (HRTEM) is recorded. Particles are highly agglomerated and tend to form stacking on to each other. The crystals were heterogeneous in size, polydisperse, well crystalline and measured from around 80 nm in diameter, bigger than estimated from the XRD. The HRTEM image of perovskite is carried out to calculate the d spacing in the LSCO lattice. HRTEM image exhibited a lattice fringe spaced by 2.72 angstrom, corresponding to the (110) plane of LSCO (Figure 2b).

Additionally, the high angle annular dark-field scanning transmission electron microscopy (HAADF-STEM) elemental mapping of the LSCO particles indicates the spatial arrangement for La, Sr, Co and O. Figure 2 shows that the HAADF image of the LSCO nanoparticles, and

the corresponding elemental mapping of La (Figure 2c), Sr (Figure 2d) and Co (Figure 2e) corroborates the existence of Sr in the crystal structure.

## 4. ELECTROCATALYTIC STUDY OF METHANOL ELECTROOXIDATION

### 4.1 Electrocatalytic activity of LSCO catalyst

After thorough characterization of the synthesized electrocatalyst, the electrocatalytic properties were studied in alkaline solution (Figure 3). Unless otherwise stated, the electrocatalytic activity by linear sweep voltammetry (LSV) and cyclic voltammetry (CV) was measured at a scan rate of 10 mV $s^{-1}$ and 40 mV $s^{-1}$ respectively, normalized by their geometric area (0.071 $cm^2$) and converted to RHE.

To understand the OER activity, the linear sweep voltammograms (LSV) and cyclic voltammograms were recorded by sweeping the potential from 1.0 V to 1.54 V in basic electrolyte. Figure 3 represents the obtained CV and LSV plot of glassy carbon/LSCO modified electrode which demonstrates the OER onset to be 1.47 V (black trace), which is also confirmed by the current response and appearance of bubbles on the electrode surface. Current density and onset potential are important indicators to evaluate the efficacy of the electrocatalyst. In presence of 0.5 M MeOH along with 0.5 M KOH, higher current density and low overpotential (red trace) were observed indicating that the catalyst has activity towards methanol electrooxidation.

To further identify the surface species formed, cyclic voltammetry studies are performed (Figure 3b). However, there is no characteristic peak observed in the specified potential range in alkaline as well as methanol contained system but some important observations were noted: (a) The electrocatalytic oxidation of methanol over LSCO modified GCE electrode was noticeable with onset at 1.34 V, as revealed in Figure 3a, this value is 130 mV lesser than alkaline system (b) 2-fold increment of current density (i.e., ~ 6 mA/$cm^2$ to ~12 mA/$cm^2$) at

same potential, in comparison with the study in alkaline medium. The increased current density and reduced onset potential clearly show the significant electrochemical reactivity of LSCO towards methanol oxidation and provide evidence that methanol addition is possibly facilitating OER.

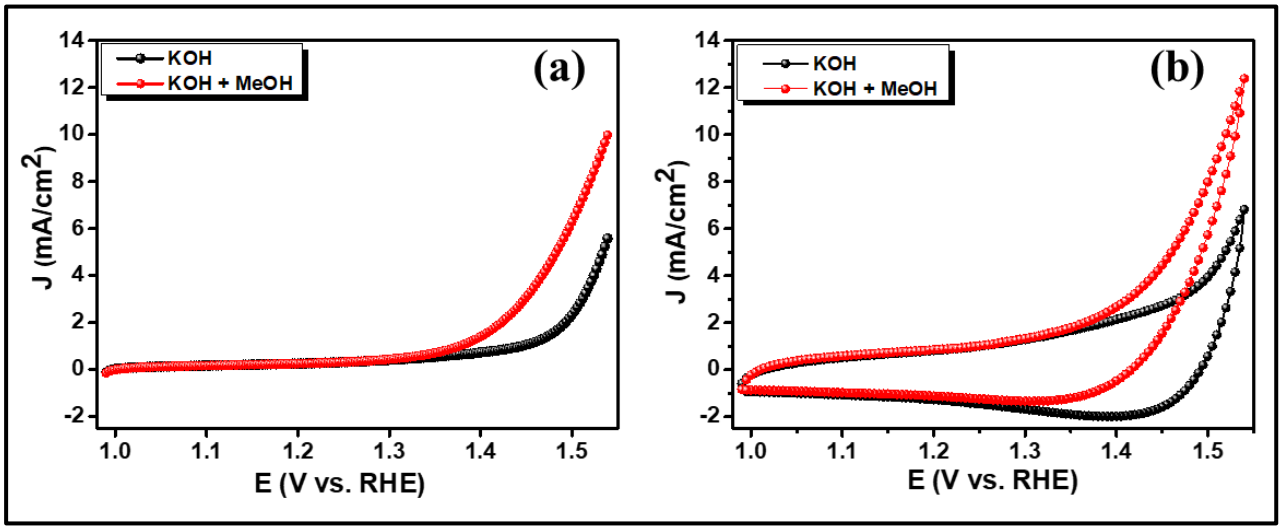


**Figure 3:** *(a) Linear sweep voltammogram, (b) Cyclic voltammogram of LSCO in 0.5 M KOH with a scan speed of 10 $mVs^{-1}$ and 40 $mVs^{-1}$. MOR of LSCO modified GCE in the mixture of 0.5 M Methanol in 0.5 M KOH solution.*

Furthermore, we monitored the methanol electrooxidation under neutral pH. In the neutral medium (0.5 M $KNO_3$) also, similar trends have been noticed for methanol electrooxidation (Figure S1). Current density and bubbling on the working electrode are indicative of the OER response. In neutral medium, onset potential is slightly shifted after addition of methanol and the current density enhances by 1.35 times. This study confirms the activity and stability of synthesized perovskite for methanol electrooxidation in both the neutral and alkaline condition. The electrochemical oxidation of $CH_3OH$ can be performed over a wide pH range covering acidic, neutral, and alkaline medium. The literature suggests several advantages in an alkaline solution such as high efficiency, facile adsorption of hydroxide ions (water molecule) to enhance the electrooxidation process even at lower potential[27,43]. Hence, in present work, we

stressed our studies extensively in alkaline medium in order to understand the methanol assisted OER mechanism.

### 4.2 Concentration dependent study and stability test

The linear sweep voltammograms for the methanol oxidation on the LSCO surface in different methanol concentrations were carried out to obtain the optimal concentration of methanol. For electrocatalytic MOR, the current density increases on increasing the concentration of methanol, their respective percent increment in current density is shown in Figure 4a. This study suggests the excellent electron transfer properties of perovskite material or the methanol electrooxidation process is mass-transfer-controlled up to 0.5 M of methanol concentration. It is well known that concentrated methanol solution is a target fuel in the DMFCs to reduce the volume. Increasing of methanol concentration can also have a negative influence on the current density[14,44], which means that the catalytic activity only increases up to a certain methanol concentration and tends to decrease after that optimum concentration. However, in our study there is no negative influence on the current density by LSCO perovskite but the increment almost levels off after 0.5 M concentration of $CH_3OH$. We speculated that it could be due to the saturation of active sites at the catalyst surface. Hence, we have performed all our studies in 0.5 M methanol contained alkaline medium in accordance with the result obtained by concentration dependent studies.

In practical applications, stability is a significant index for the durability of an electrocatalyst. Time dependent activity and the stability of perovskite modified electrode is probed by chronoamperometry (CA) measurements. These are evaluated by steady state electrocatalysis at constant applied potential of 1.54 V vs. RHE over 1800 s (Figure 4a). Chronoamperometry shows a typical response where the current density first rises and drops reaching a steady state within 1800 seconds. After 1800 seconds, the current is ~ 2.0 $mA/cm^2$ and 5.0 $mA/cm^2$ for

LSCO in 0.5 M KOH and 0.5 M KOH + 0.5 M MeOH contained electrolyte. Steady-state stability tests confirmed that the catalyst remained highly active throughout the prolonged operation of constant potential. Moreover, the stability of the catalyst is tested by characterising via XRD and FESEM. The chronoamperometry test was performed at 1.54 V in the methanol contained KOH electrolyte (Figure S3). A comparison between the as synthesised catalyst (Pre) and after electrocatalysis (Post) shows no apparent bulk changes, confirming the stability of the material (Figure S8). SEM images shows slight change in morphology as catalyst was exposed to methanol containing electrolyte and as gases evolved during methanol electrooxidation (Figure S9). Inductively coupled mass spectrometry (ICP-MS) analysis (Table S1) indicated only 0.004% dissolution of all the metal elements (Sr and Co) collectively, which ensured that there is minimal to no element dissolution of catalyst component post electrolysis.

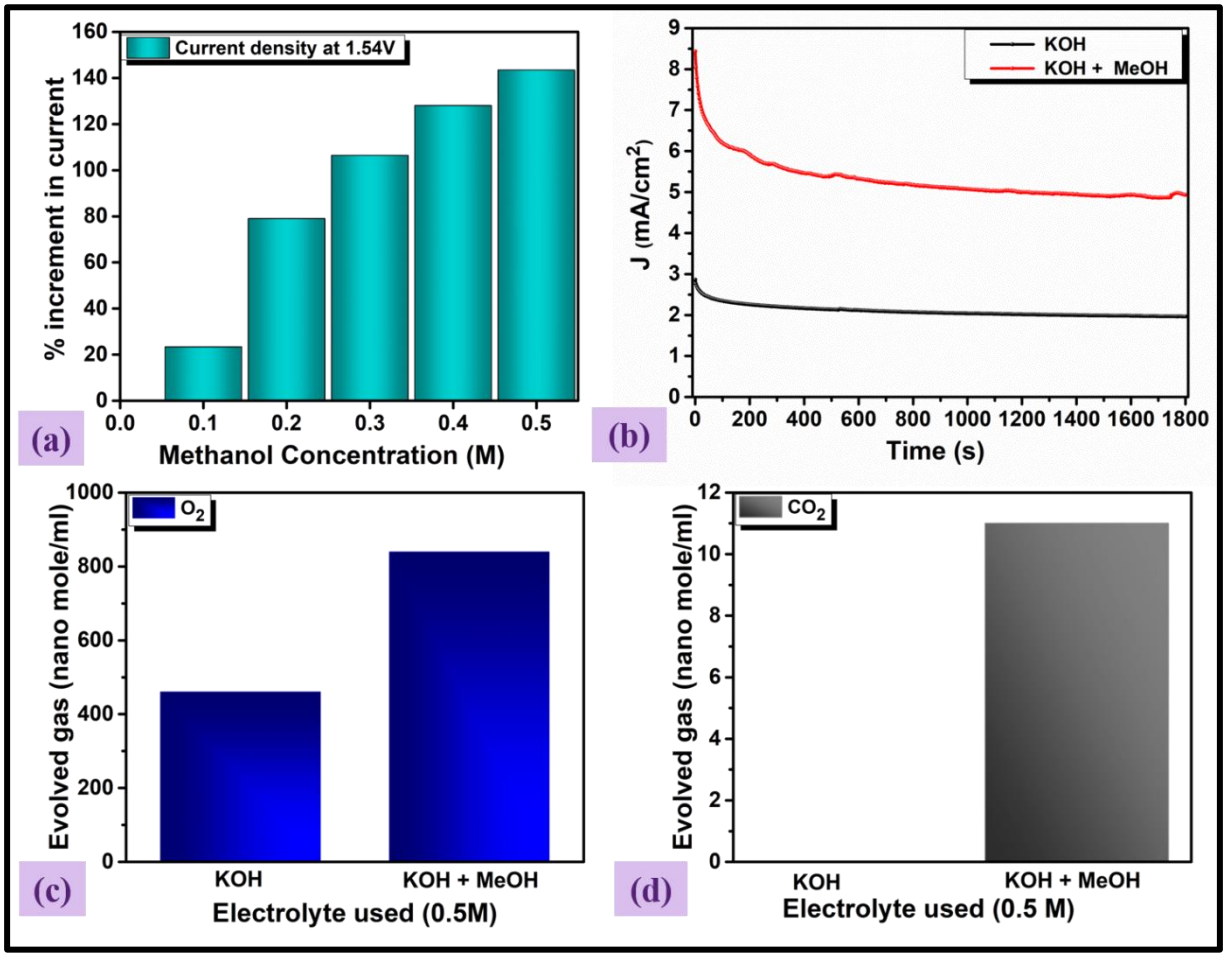

**Figure 4:** *(a) Chronoamperometry profile at constant potential of 1.54 V in KOH and methanol medium. (b) Dependence of methanol (% increment in current) oxidation on concentration of methanol. The trend of (**c**) Oxygen and (d) Carbon dioxide accumulation in the headspace of the air-tight container.*

### 4.3 Gaseous product analysis

In order to corroborate that oxidation current is indeed due to methanol oxidation, quantitative analysis of the product gases resulting from CA experiment (1.54 V for 1800 s) is carried out in Gas Chromatograph. During the CA experiment the gases sampled in the head space of the closed electrochemical cell (1 ml of gas was taken) were collected and subjected to gas chromatography. It is evident from Figure 4c that on addition of methanol, OER enhances from 460 nano moles/ml to 840 nano moles/ml. Thus, in presence of methanol rate of OER increases to almost double confirming the assisted OER in presence of methanol electrooxidation.

We employed a long Chronoamperometry (CA) study to measure the evolved oxygen during the water electrooxidation and methanol assisted water electrooxidation process. The leak proof three-electrode electrochemical setup was involved during the 6-hour CA experiment and the evolution of oxygen moles over time sampled in the head space of the closed electrochemical cell (1 ml of gas was taken) were collected and subjected to gas chromatograph in 30-minute interval. Figure S3 (b) clearly demonstrate that the oxygen mole increased progressively throughout the reaction duration for both the process and a significant increase in the oxygen mole with time during methanol electrooxidation compared to water electrooxidation.

Along with this, $CO_2$ was also detected in measurable amount in some set of experiments and no trace of CO was detected in flame ionization detector. Further, the presence of formic acid detected by NMR over an extended period of time strongly indicates that the oxidation of methanol is taking place through the formate pathway. This finding provides compelling evidence for the complete conversion of methanol via this specific pathway[43,45].

### 4.4 RRDE voltametric investigation: Validation of MeOH assisted OER mechanism:

### *4.4.1 Behaviour of the disk electrode*

Hydrodynamic voltametric technique was employed to validate the methanol assisted oxygen evolution reaction (OER) in KOH medium. The advantage of the RRDE setup used in this work hinges on the selective reduction of oxygen evolved by the GC disk electrode over the Au ring electrode[47]. Here, we have performed linear sweep voltammetry (LSV) at the GC disk electrode in the potential window for OER by sweeping the potential from 1.0 V to 1.7 V at a scan rate of 5 mV $s^{-1}$ and simultaneously we have done chronoamperometry (CA) on the Au ring electrode by applying a constant bias of 0.7 V vs. RHE to ensure efficient $O_2$ reduction. (Figure 5). RRDE studies demonstrate that the OER in methanol contained system starts at a potential which is 100 mV lower than pure KOH electrolyte, proving the assisted OER in presence of methanol (Figure 5a, b). These results are in agreement with studies done on glassy carbon electrode in non-hydrodynamic condition. Here, methanol electrooxidation is a mass transfer process because it is dissolved in a reasonably small concentration (0.5 M). On the other hand, water is in large abundance so it is a kinetically controlled process. We measured the charge associated with each system to further support the methanol assisted water electrooxidation. Charge is calculated by chronoamperometric analysis (Figure 5c) at ring electrode by maintaining 0.7 V vs. RHE on the Au ring while maintaining the disk electrode at 1.6 V vs. RHE in 0.5 M KOH medium and methanol contained electrolyte medium. It is clearly observed that, charge associated in alkaline medium is 2.04 mC which enhanced to 5.06 mC in methanol contained electrolyte system (Figure 5d).

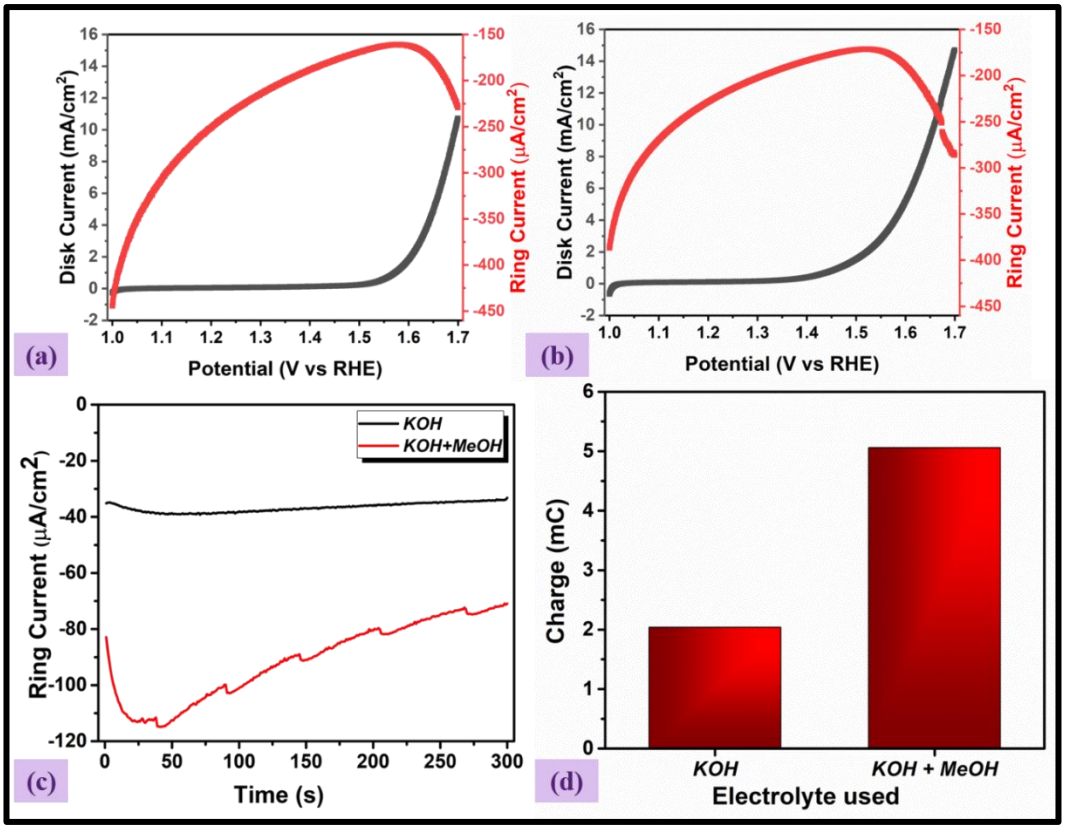


**Figure 5:** *RRDE measurement of LSCO during OER at the disk and by holding the potential at 0.7 V vs. RHE in the Au ring in (a) 0.5 M KOH medium and (b) methanol (0.5 M) contained in 0.5 M KOH medium. (c) Chronoamperometric analysis at ring electrode by maintaining 0.7 V vs. RHE on the Au ring while maintaining the disk electrode at 1.6 V vs. RHE in 0.5 M KOH medium and methanol contained electrolyte medium. (d) Charge associated with the chronoamperometric studies.*

### *4.4.2 Behaviour of the ring electrode*

Generally, in RRDE technique, LSV is done on the disk and the ring is biased at such a potential where the product formed on the disk during the LSV would get reduced/oxidized back to another product thus giving a negative/positive ring current respectively. Thus, until the specific reaction does not start on the disk electrode, the ring current should be zero or very low as there is no product which the ring would reduce/oxidize. In our case, the product formed on the disk during LSV is oxygen due to water oxidation so the ring must show a reduction current only when the disk potential crosses the water oxidation regime (in this case around

1.52 V). But surprisingly, we observed that the ring current (reduction current) is very pronounced (- 444 μA/cm$^2$) right in the beginning itself where there is no water oxidation occurring. To emphasize further, even when the applied potential is just 1.0 V and the oxygen evolution reaction has not yet started, significant reduction on the ring is noticed (red curve in Figure 5a). Similar behaviour is also observed when we performed the experiment in methanol containing electrolyte medium (red curve in Figure 5b).

Some major observations and conclusions from Figure 5 are: (a) reduction in the oxygen reduction onset voltage in presence of methanol (b) ring current (reduction current shown as the red curve) is pronounced before the reaction. Point (a) gives us clear validation of methanol assisted OER as the onset for the reduction current on the ring electrode was observed at -1.50 V vs. RHE in presence of methanol (Figure 5a) while the same is -1.57 V vs RHE without methanol (Figure 5b). Point (b) Ring current is very pronounced even in alkaline and methanol contained electrolyte system, which confirms the reduction of the catalyst's lattice oxygen because even without OER, significant reduction current is generated on the ring so it has to be the lattice oxygen from LSCO whose reduction is going on at the ring.

**4.5 Does Lattice Oxygen evolved during the reaction?**

Bisht et al.[48] and Yadav et al.[37] have demonstrated via $H_2$ TPR studies that the substitution of Sr improves the lattice oxygen exchange properties and the reducibility of the $LaCoO_3$. As mentioned, ring current is very pronounced even at the start of the experiment, which provide evidence of the reduction of lattice oxygen. In order to verify if this is indeed happening, we first reduced the catalyst (LSCO) to prepare R-LSCO catalyst in order to utilize the lattice oxygen present in the system (Figure 5c). Clearly, from Figure 5c, it is evident that the ring current for ORR is almost negligible in the case of R-LSCO as compared to fresh LSCO catalyst. Thus, the reduced catalyst, which is deficient in the lattice oxygen show less reduction

current on the ring and this proves that the ring current before OER is indeed due to the lattice oxygen from the catalyst. It is noticeable that the activity of R-LSCO is not very different from the original LSCO thus, lattice oxygen may not have any role in alerting the catalyst's activity.

Lattice oxygen behavior is further validated by running a control experiment with Pt/C in the same experimental condition (Figure 6b). Please note that Pt/C is free from any lattice oxygen and should show insignificant reduction current before OER starts and it is clear from Figure 6b that there is only -26 $\mu A/cm^2$ in the potential range of 1.0 V to 1.5 V. The current enhances to - 43 $\mu A/cm^2$ post 1.5 V where the reaction enters the OER regime i.e., 1.55 V. This control experiment clearly confirms that lattice oxygen evolves from perovskite catalyst and the reduction current in Figure 5a and Figure 5b is solely from lattice oxygen.

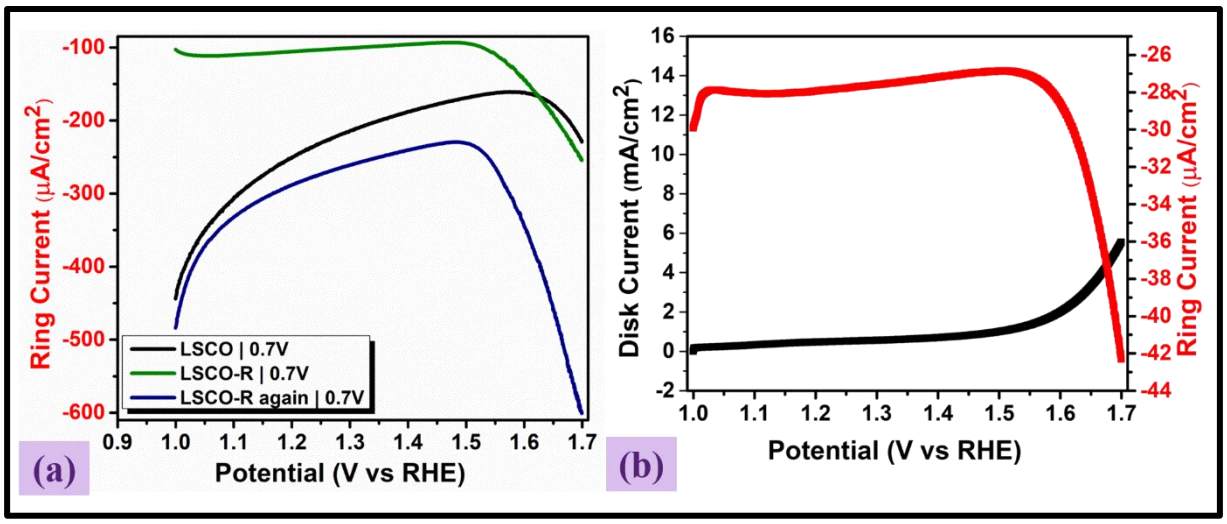


**Figure 6:** *(a) RRDE measurements during OER at the ring using LSCO catalyst by biasing the Au ring at 0.7V vs. RHE for fresh catalyst (Black trace), reduced catalyst (Olive trace), again scan on catalyst after OER (Blue trace) for ORR at 1600 rpm. (b) RRDE measurement of Pt/C during OER at the disk and by holding the potential at 0.7 V vs. RHE in the Au ring contained in 0.5 M KOH medium.*

### 4.6 Exchange of lattice oxygen with the solvent

Heterogeneous electrocatalysis over metal oxide generally occur via the Mars and van Krevelen (MVK) mechanism[49], where reductant reacts with the surface oxygen of the metal oxide. In our

case, there's possibility that while oxygen evolution is occurring, oxygen vacancies/defects are generated on catalyst surface due to lattice oxygen removal. These defects are filled up by solvent or gaseous phase molecular oxygen, indicating dynamic exchange of oxygen. To further corroborate the dynamic exchange behavior, we scanned the R-LSCO electrode again after keeping it in the electrolyte for some time. Interestingly, the original electrochemical behaviour is attained as evident by blue trace in Figure 6a. Overall, the RRDE studies confirms the evolution of lattice oxygen, exchange of lattice oxygen with the solvent and the methanol assisted water oxidation reaction.

## 5. Elevated Oxygen Evolution Reaction via Adsorption-Mediated Kinetics:

***5.1 Surface chemistry in the unbiased condition*:** The OCP of a working electrode is its potential measured versus a reference electrode when no external current flows, i.e., unbiased condition. The OCP is an important parameter in the study of electrode processes and is related to the equilibrium between the catalytic surface and the electrolyte.

The OCP across the WE (LSCO/GCE modified electrode) and reference electrode was measured as a function of time in KOH and KOH + methanol. The measurements were performed for a total duration of 40,000 seconds. It was observed that in the KOH medium the OCP exhibits non steady state behaviour (Figure 7 a,b). First, the potential rises in the KOH medium as a result of $OH^-$ being adsorbed onto the catalyst surface. The system was kept running for about 6000 seconds still the saturation potential could not be obtained. Thus, there is a strong possibility that a dynamic exchange of some reactive species (lattice oxygen) from the catalyst's surface is occurring. RRDE experiments have already validated this phenomenon. Briefly, lattice oxygen leaves the surface at OCP and hydroxyls get adsorbed on the vacancy thus created. Due to this dynamic exchange, equilibrium is not attained within the timeframe of the experiment and a continuous rise in the potential happens. Cleary, this is an oxidation process and lattice oxygen removal justifies this as per the reaction; $O^{2-} \rightarrow 1/2O_2$ . To validate

this further, we investigated the OCP behaviour of Pt wire (Figure S2). OCP behaviour from Figure S2 suggest that due to the absence of dynamic exchange of lattice oxygen in Pt metal, equilibrium is quickly reached and OCP becomes saturated.

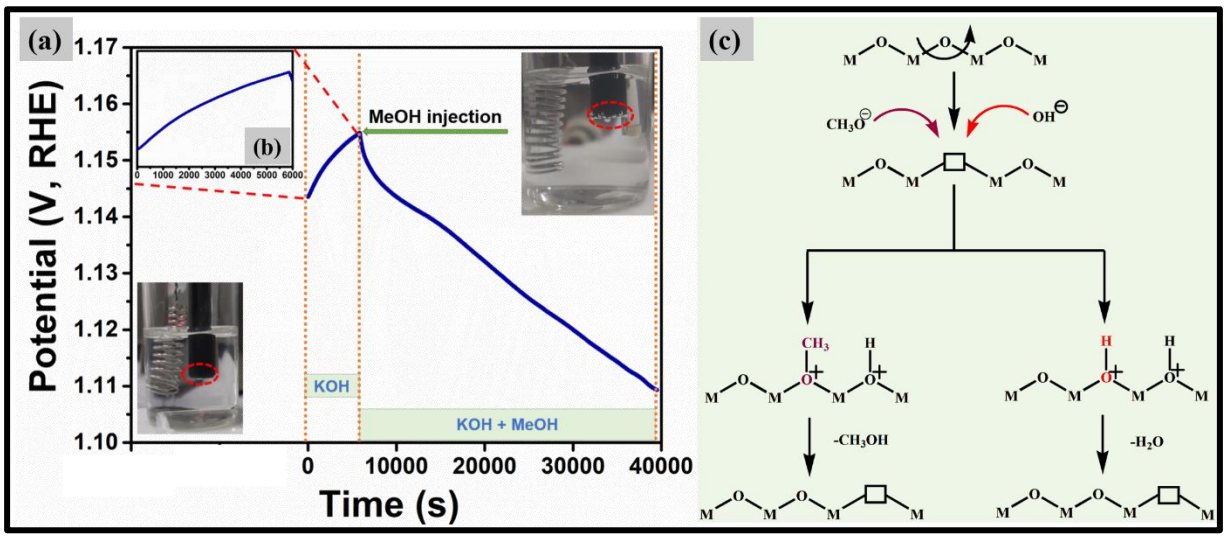


**Figure 7***: (a) OCP vs time plot for LSCO catalyst in the presence of 0.5M KOH (until 6000 sec)* and *0.5M KOH + 0.5M MeOH contained electrolyte. (b) is magnified view of OCP profile in a time frame till 6000 sec (c) Representation of proposed mechanism at unbiased condition (OCP). (b) OCP vs time plot for LSCO catalyst in the presence of 0.5M KOH (until 6000 sec)* and *0.5M KOH + 0.5M MeOH contained electrolyte.*

Once the methanol is added, potential tends to decrease as dynamic exchange is diminished as a result of methanol adsorption (Figure 7a). The schematic representation of reaction occurring at unbiased condition is mentioned in Figure 7c.

***5.2 Surface chemistry in the biased condition:*** It is known that hydroxide adsorbed on catalyst surface are utilized for MeOH electrooxidation prior to OER and ultimately once the potential crosses the OER regime, adsorbed $OH^-$ also participates for OER. Thus, $OH^-$ is the common reactive species for OER as well methanol. Both OER and methanol electro-oxidation occurs using hydroxyls as per69 the following reactions:

$$CH_3OH + 6OH^- \rightarrow CO_2 + 5\,H_2O + 6e^-$$

$$2OH^- \rightarrow O_2 + 2H^+ + 4e^-$$

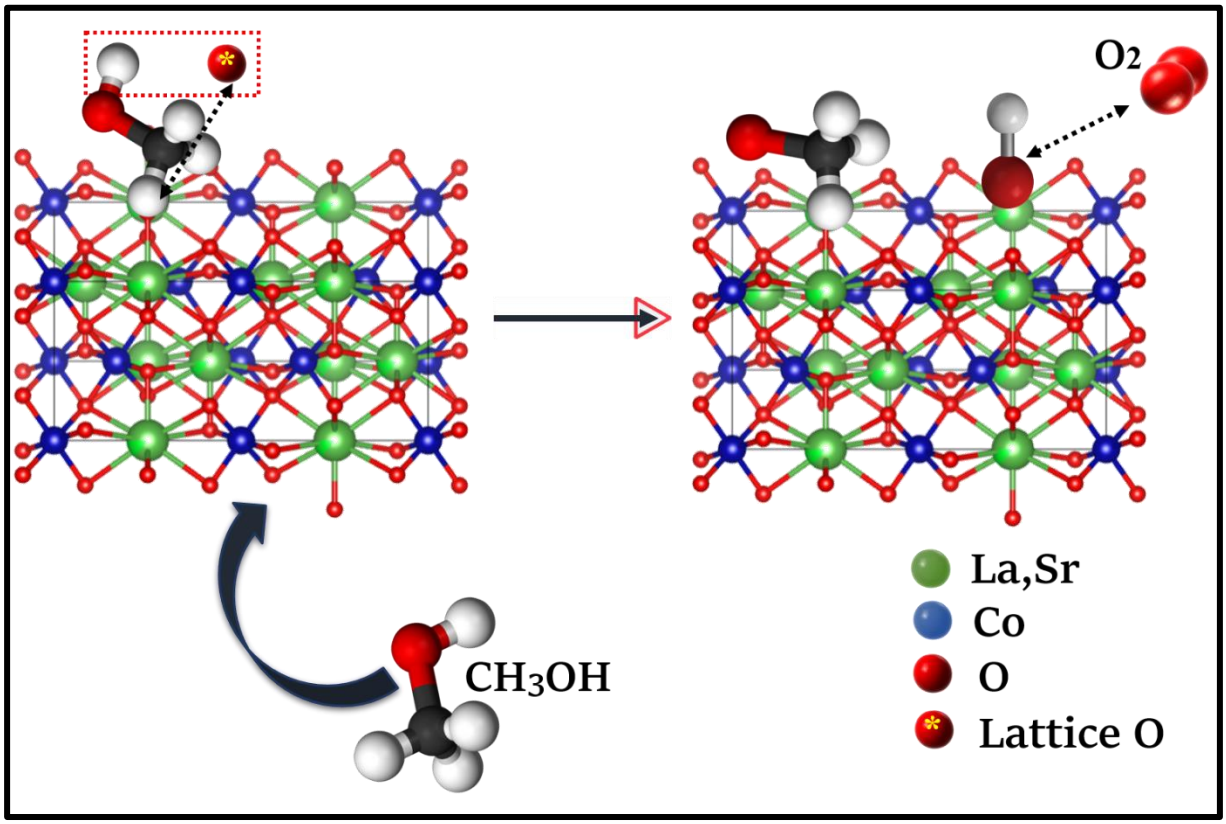


**Figure 8:** *Schematic illustration of surface chemistry of methanol electrooxidation in the biased condition: This schematic illustration depicts the surface chemistry of methanol electrooxidation over catalyst surface via dissociative chemisorption pathway.*

One can now explain the elevated OER in presence of methanol. Methanol chemisorbs dissociative onto the LSCO surface as methoxy and hydroxyl[46] (Figure 8). After this chemisorption, methanol oxidizes utilizing hydroxyl to form $CO_2$ via formate route as stated earlier. Thus, one can anticipate that methanol adsorption creates hydroxyls over the surface in addition to the hydroxyls forming during OER and in this way concentration of hydroxyls increase as a result of methanol adsorption. Clearly, the OER rate increases in presence of methanol due to enhanced hydroxyls concentration. Thus, the enhanced OER in presence of methanol is purely a kinetic phenomenon and can be simply termed as the methanol assisted water oxidation.

## 5 CONCLUSION

The observations reported herein investigate the methanol assisted water oxidation using a noble metal free LSCO perovskite in alkaline medium at near thermodynamic potential. There are several experimental evidences that points to the fact that rate of OER enhances both in alkaline and the neutral medium in presence of methanol. Clearly, this confirms that methanol assists the water oxidation process. Quantitatively, the moles of evolved oxygen are 460 nanomoles/ml in KOH and 840 nanomoles/ml in KOH + methanol. Similar enhancement is also noticed in the electro-oxidation current. RRDE experiments provide a very important insight into the assisted water oxidation as well as the catalyst's behaviour. RRDE demonstrate that the onset of oxygen reduction decreases by 70 mV on presence of methanol, another evidence of methanol assisted water oxidation. Interestingly, ring current demonstrate that LSCO catalysts exchanges the lattice oxygen with the aqueous electrolyte which opens a new dimension on the applicability of RRDE experimentation. A detailed study on the open circuit potential (OCP) study explains the adsorption behaviour of KOH and methanol. By the OCP study it is established that the main reason behind the elevated OER phenomenon is the enhanced concentration of hydroxyls due to methanol chemisorption; a kinetic effect.

## AUTHOR INFORMATION

**Shikha Dhakar-** Department of Chemistry, Indian Institute of Technology Gandhinagar, Gujarat-382355

**Sanchayita Mukhopadhyay-** Department of Chemistry, Indian Institute of Science Education and Research, Pune, Maharashtra 411008, India

**Musthafa Ottakam Thotiyl-** Department of Chemistry, Indian Institute of Science Education and Research, Pune, Maharashtra 411008, India

**Sudhanshu Sharma-** Department of Chemistry, Indian Institute of Technology Gandhinagar, Gujarat-382355

orcid.org/0000-0002-5217-9941; Email: ssharma@iitgn.ac.in

## SUPPORING INFORMATION

Electrocatalysis supporting results as MOR studies in $KNO_3$ medium, iR drop corrected data, Long chronoamperometry data, trend of oxygen accumulation for 6 hours, OCP profile. TEM images, Calculation of average crystallite size and Collection efficiency. Post reaction characterization.

## ACKNOWLEDGEMENTS

SS acknowledges DST (DST/P0117/1092) and MHRD (STARS/APR2019/CS/215/FS) projects for the funding and fellowship. SD is thankful for the support from IITGN for the fellowship. M.O.T. is indebted to DST-WTI and DST-SERB for financial support.

### Conflict of interests

The authors declare no intellectual as well as financial conflict of interests.

## 6 REFERENCE

(1) Hoque, N.; Baruah, M. J.; Biman, A. H.; Biswas, S.; Gogoi, G.; Dutta, R.; Bania, K. K. Impregnating Rhodium(0) Sites through Zeolite-Y Templation in a Hybrid Rh–Ni Catalyst for Alcohol Electro-Oxidation with Low CO Poisoning. *ACS Appl. Energy Mater.* **2022**, *5* (5), 6118–6128. https://doi.org/10.1021/acsaem.2c00523.

(2) Subbaraman, R.; Tripkovic, D.; Chang, K.-C.; Strmcnik, D.; Paulikas, A. P.; Hirunsit, P.; Chan, M.; Greeley, J.; Stamenkovic, V.; Markovic, N. M. Trends in Activity for the Water Electrolyser Reactions on 3d M(Ni,Co,Fe,Mn) Hydr(Oxy)Oxide Catalysts. *Nat Mater* **2012**, *11* (6), 550–557. https://doi.org/10.1038/nmat3313.

(3) Putra, R. P.; Horino, H.; Rzeznicka, I. I. An Efficient Electrocatalyst for Oxygen Evolution Reaction in Alkaline Solutions Derived from a Copper Chelate Polymer via In-Situ Electrochemical Transformation. **2020**.

(4) Liu, W.; Xie, J.; Guo, Y.; Lou, S.; Gao, L.; Tang, B. Sulfurization-Induced Edge Amorphization in Copper–Nickel–Cobalt Layered Double Hydroxide Nanosheets Promoting Hydrazine Electro-Oxidation. *J. Mater. Chem. A* **2019**, *7* (42), 24437–24444. https://doi.org/10.1039/C9TA07857F.

(5) Song, J.; Wei, C.; Huang, Z.-F.; Liu, C.; Zeng, L.; Wang, X.; Xu, Z. J. A Review on Fundamentals for Designing Oxygen Evolution Electrocatalysts. *Chem. Soc. Rev.* **2020**, *49* (7), 2196–2214. https://doi.org/10.1039/C9CS00607A.

(6) Bender, M. T.; Lam, Y. C.; Hammes-Schiffer, S.; Choi, K.-S. Unraveling Two Pathways for Electrochemical Alcohol and Aldehyde Oxidation on NiOOH. *J. Am. Chem. Soc.* **2020**, *142* (51), 21538–21547. https://doi.org/10.1021/jacs.0c10924.
(7) Wei, X.; Li, Y.; Chen, L.; Shi, J. Formic Acid Electro-Synthesis by Concurrent Cathodic CO2 Reduction and Anodic CH3OH Oxidation. *Angewandte Chemie* **2021**, *133* (6), 3185–3192. https://doi.org/10.1002/ange.202012066.
(8) Liu, Y.; Zhao, S.-F.; Guo, S.-X.; Bond, A. M.; Zhang, J.; Zhu, G.; Hill, C. L.; Geletii, Y. V. Electrooxidation of Ethanol and Methanol Using the Molecular Catalyst [{Ru4O4(OH)2(H2O)4}(γ-SiW10O36)2]10–. *J. Am. Chem. Soc.* **2016**, *138* (8), 2617–2628. https://doi.org/10.1021/jacs.5b11408.
(9) Simon Araya, S.; Liso, V.; Cui, X.; Li, N.; Zhu, J.; Sahlin, S. L.; Jensen, S. H.; Nielsen, M. P.; Kær, S. K. A Review of The Methanol Economy: The Fuel Cell Route. *Energies* **2020**, *13* (3), 596. https://doi.org/10.3390/en13030596.
(10) Li, L.; Gao, W.; Wan, X.; Wen, D. Pt Nanoparticles Dispersed on Ni/C Nanoflowers as Stable Electrocatalysts for Methanol Oxidation and Oxygen Reduction. *ACS Appl. Nano Mater.* **2021**. https://doi.org/10.1021/acsanm.1c02427.
(11) Wang, Y.; Wang, S.; Li, F.; Wang, Y.; Zhang, H.; Sun, C. Pt Nanoparticles Loaded on W18O49 Nanocables–RGO Nanocomposite as a Highly Active and Durable Catalyst for Methanol Electro-Oxidation. *ACS Omega* **2018**, *3* (12), 16850–16857. https://doi.org/10.1021/acsomega.8b02942.
(12) Chen, Z.; He, Y.-C.; Chen, J.-H.; Fu, X.-Z.; Sun, R.; Chen, Y.-X.; Wong, C.-P. PdCu Alloy Flower-like Nanocages with High Electrocatalytic Performance for Methanol Oxidation. *J. Phys. Chem. C* **2018**, *122* (16), 8976–8983. https://doi.org/10.1021/acs.jpcc.8b01095.
(13) Radhakrishnan, T.; Sandhyarani, N. Pt-Ag Nanostructured 3D Architectures: A Tunable Catalyst for Methanol Oxidation Reaction. *Electrochimica Acta* **2019**, *298*, 835–843. https://doi.org/10.1016/j.electacta.2018.12.151.
(14) Barakat, N. A.; Abdelkareem, M. A.; El-Newehy, M.; Kim, H. Y. Influence of the Nanofibrous Morphology on the Catalytic Activity of NiO Nanostructures: An Effective Impact toward Methanol Electrooxidation. *Nanoscale Research Letters* **2013**, *8* (1), 402. https://doi.org/10.1186/1556-276X-8-402.
(15) Zhao, S.; Yang, H.; Liu, Y.; Xing, Y.; Cui, G.; Liu, Q. Cu-Doped Co3O4 Microstructure as an Efficient Non-Noble Metal Electrocatalyst for Methanol Oxidation in a Basic Solution. *New J. Chem.* **2021**, *45* (25), 11245–11252. https://doi.org/10.1039/D1NJ01953H.
(16) Kaur, B.; Srivastava, R.; Satpati, B. Highly Efficient CeO2 Decorated Nano-ZSM-5 Catalyst for Electrochemical Oxidation of Methanol. *ACS Catal.* **2016**, *6* (4), 2654–2663. https://doi.org/10.1021/acscatal.6b00525.
(17) Royer, S.; Duprez, D.; Can, F.; Courtois, X.; Batiot-Dupeyrat, C.; Laassiri, S.; Alamdari, H. Perovskites as Substitutes of Noble Metals for Heterogeneous Catalysis: Dream or Reality. *Chem. Rev.* **2014**, *114* (20), 10292–10368. https://doi.org/10.1021/cr500032a.
(18) Beall, C. E.; Fabbri, E.; Schmidt, T. J. Perovskite Oxide Based Electrodes for the Oxygen Reduction and Evolution Reactions: The Underlying Mechanism. *ACS Catal.* **2021**, *11* (5), 3094–3114. https://doi.org/10.1021/acscatal.0c04473.
(19) Park, N.-G. Perovskite Solar Cells: An Emerging Photovoltaic Technology. *Materials Today* **2015**, *18* (2), 65–72. https://doi.org/10.1016/j.mattod.2014.07.007.
(20) Miao, X.; Wu, L.; Lin, Y.; Yuan, X.; Zhao, J.; Yan, W.; Zhou, S.; Shi, L. The Role of Oxygen Vacancies in Water Oxidation for Perovskite Cobalt Oxide Electrocatalysts: Are More

Better? *Chemical Communications* **2019**, *55* (10), 1442–1445. https://doi.org/10.1039/C8CC08817A.
(21) Bie, S.; Zhu, Y.; Su, J.; Jin, C.; Liu, S.; Yang, R.; Wu, J. One-Pot Fabrication of Yolk–Shell Structured La0.9Sr0.1CoO3 Perovskite Microspheres with Enhanced Catalytic Activities for Oxygen Reduction and Evolution Reactions. *J. Mater. Chem. A* **2015**, *3* (44), 22448–22453. https://doi.org/10.1039/C5TA05271H.
(22) Tomar, A. K.; Pan, U. N.; Kim, N. H.; Lee, J. H. Enabling Lattice Oxygen Participation in a Triple Perovskite Oxide Electrocatalyst for the Oxygen Evolution Reaction. *ACS Energy Lett.* **2023**, *8* (1), 565–573. https://doi.org/10.1021/acsenergylett.2c02617.
(23) Bisht, A.; Yadav, P. K.; Dhakar, S.; Sharma, S. Pt4+ as an Active Site for Oxygen Evolution Reaction in La1–XSrxCo1–YPtyO3. *J. Phys. Chem. C* **2021**, *125* (46), 25488–25496. https://doi.org/10.1021/acs.jpcc.1c06426.
(24) Mekazni, D. S.; Arán-Ais, R. M.; Ferre-Vilaplana, A.; Herrero, E. Why Methanol Electro-Oxidation on Platinum in Water Takes Place Only in the Presence of Adsorbed OH. *ACS Catal.* **2022**, *12* (3), 1965–1970. https://doi.org/10.1021/acscatal.1c05122.
(25) Qian, K.; Li, L.; Chen, P.; Xiu, Y.; E, Y.; Gies, H. Copper-Nickel Doped LTA Zeolite as a High- Efficiency Methanol Oxidation Reaction Catalyst in Alkaline Solution. *International Journal of Hydrogen Energy* **2021**, *46* (46), 23898–23905. https://doi.org/10.1016/j.ijhydene.2021.04.155.
(26) Zhu, J.; Xia, L.; Yu, R.; Lu, R.; Li, J.; He, R.; Wu, Y.; Zhang, W.; Hong, X.; Chen, W.; Zhao, Y.; Zhou, L.; Mai, L.; Wang, Z. Ultrahigh Stable Methanol Oxidation Enabled by a High Hydroxyl Concentration on Pt Clusters/MXene Interfaces. *J. Am. Chem. Soc.* **2022**, *144* (34), 15529–15538. https://doi.org/10.1021/jacs.2c03982.
(27) Rus, E. D.; Wakabayashi, R. H.; Wang, H.; Abruña, H. D. Methanol Oxidation at Platinum in Alkaline Media: A Study of the Effects of Hydroxide Concentration and of Mass Transport. *ChemPhysChem* **2021**, *22* (13), 1397–1406. https://doi.org/10.1002/cphc.202100087.
(28) Mahapatra, S. S.; Datta, J. Characterization of Pt-Pd/C Electrocatalyst for Methanol Oxidation in Alkaline Medium. *International Journal of Electrochemistry* **2011**, *2011*, e563495. https://doi.org/10.4061/2011/563495.
(29) Yoo, J. S.; Rong, X.; Liu, Y.; Kolpak, A. M. Role of Lattice Oxygen Participation in Understanding Trends in the Oxygen Evolution Reaction on Perovskites. *ACS Catal.* **2018**, *8* (5), 4628–4636. https://doi.org/10.1021/acscatal.8b00612.
(30) Fabbri, E.; Schmidt, T. J. Oxygen Evolution Reaction—The Enigma in Water Electrolysis. *ACS Catal.* **2018**, *8* (10), 9765–9774. https://doi.org/10.1021/acscatal.8b02712.
(31) Mefford, J. T.; Rong, X.; Abakumov, A. M.; Hardin, W. G.; Dai, S.; Kolpak, A. M.; Johnston, K. P.; Stevenson, K. J. Water Electrolysis on La1−xSrxCoO3−δ Perovskite Electrocatalysts. *Nat Commun* **2016**, *7* (1), 11053. https://doi.org/10.1038/ncomms11053.
(32) Mehboob, A.; Gilani, S. R.; Anwar, A.; Sadiqa, A.; Akbar, S.; Patujo, J. Nanoscale Cobalt-Oxide Electrocatalyst for Efficient Oxygen Evolution Reactions in Alkaline Electrolyte. *J Appl Electrochem* **2021**, *51* (4), 691–702. https://doi.org/10.1007/s10800-021-01529-1.
(33) Sharma, S.; Mukri, B. D.; Hegde, M. S. Direct Evidence of Redox Interaction between Metal Ion and Support Oxide in Ce0.98Pd0.02O2−δ by a Combined Electrochemical and XPS Study. *Dalton Trans.* **2011**, *40* (43), 11480–11489. https://doi.org/10.1039/C1DT11262G.

(34) Zhu, Y.; Zhou, W.; Yu, J.; Chen, Y.; Liu, M.; Shao, Z. Enhancing Electrocatalytic Activity of Perovskite Oxides by Tuning Cation Deficiency for Oxygen Reduction and Evolution Reactions. *Chem. Mater.* **2016**, *28* (6), 1691–1697. https://doi.org/10.1021/acs.chemmater.5b04457.
(35) Lu, Y.; Ma, A.; Yu, Y.; Tan, R.; Liu, C.; Zhang, P.; Liu, D.; Gui, J. Engineering Oxygen Vacancies into LaCoO3 Perovskite for Efficient Electrocatalytic Oxygen Evolution. *ACS Sustainable Chem. Eng.* **2019**, *7* (3), 2906–2910. https://doi.org/10.1021/acssuschemeng.8b05717.
(36) Hardin, W. G.; Mefford, J. T.; Slanac, D. A.; Patel, B. B.; Wang, X.; Dai, S.; Zhao, X.; Ruoff, R. S.; Johnston, K. P.; Stevenson, K. J. Tuning the Electrocatalytic Activity of Perovskites through Active Site Variation and Support Interactions. *Chem. Mater.* **2014**, *26* (11), 3368–3376. https://doi.org/10.1021/cm403785q.
(37) Yadav, P. K.; Kumari, S.; Naveena, U.; Deshpande, P. A.; Sharma, S. Insights into the Substitutional Chemistry of La1−xSrxCo1−yMyO3 (M = Pd, Ru, Rh, and Pt) Probed by in Situ DRIFTS and DFT Analysis of CO Oxidation. *Applied Catalysis A: General* **2022**, *643*, 118768. https://doi.org/10.1016/j.apcata.2022.118768.
(38) Sharma, S.; Singh, P.; Hegde, M. S. Electrocatalysis and Redox Behavior of Pt2+ Ion in CeO2 and Ce0.85Ti0.15O2: XPS Evidence of Participation of Lattice Oxygen for High Activity. *J Solid State Electrochem* **2011**, *15* (10), 2185–2197. https://doi.org/10.1007/s10008-011-1402-z.
(39) Vyas, D.; Sharma, S. Noble Metal-Free La0.80Sr0.20CoO3 Thin Film Electrode for Sodium Formate Electrooxidation. *Journal of Electroanalytical Chemistry* **2022**, *915*, 116327. https://doi.org/10.1016/j.jelechem.2022.116327.
(40) Sharma, S.; Hegde, M. S. Pt Metal-CeO2 Interaction: Direct Observation of Redox Coupling between Pt0/Pt2+/Pt4+ and Ce4+/Ce3+ States in Ce0.98Pt0.02O2−δ Catalyst by a Combined Electrochemical and x-Ray Photoelectron Spectroscopy Study. *J. Chem. Phys.* **2009**, *130* (11), 114706. https://doi.org/10.1063/1.3089666.
(41) Amin, H. M. A.; Königshoven, P.; Hegemann, M.; Baltruschat, H. Role of Lattice Oxygen in the Oxygen Evolution Reaction on Co3O4: Isotope Exchange Determined Using a Small-Volume Differential Electrochemical Mass Spectrometry Cell Design. *Anal. Chem.* **2019**, *91* (20), 12653–12660. https://doi.org/10.1021/acs.analchem.9b01749.
(42) Lal, B.; Raghunandan, M. K.; Gupta, M.; Singh, R. N. Electrocatalytic Properties of Perovskite-Type La1-XSrxCoO3(0⩽x⩽0.4) Obtained by a Novel Stearic Acid Sol–Gel Method for Electrocatalysis of O2 Evolution in KOH Solutions. *International Journal of Hydrogen Energy* **2005**, *7* (30), 723–729. https://doi.org/10.1016/j.ijhydene.2004.07.002.
(43) Meenu, P. C.; Roy, S.; Chakraborty, C.; Roy, S. Electro Catalytic Oxidation Reactions for Harvesting Alternative Energy over Non Noble Metal Oxides: Are We a Step Closer to Sustainable Energy Solution? *Advanced Powder Technology* **2021**, *32* (8), 2663–2689. https://doi.org/10.1016/j.apt.2021.06.018.
(44) Salarizadeh, P.; Askari, M. B.; Di Bartolomeo, A. MoS2/Ni3S2/Reduced Graphene Oxide Nanostructure as an Electrocatalyst for Alcohol Fuel Cells. *ACS Appl. Nano Mater.* **2022**, *5* (3), 3361–3373. https://doi.org/10.1021/acsanm.1c03946.
(45) Wala, M.; Simka, W. Effect of Anode Material on Electrochemical Oxidation of Low Molecular Weight Alcohols—A Review. *Molecules* **2021**, *26* (8), 2144. https://doi.org/10.3390/molecules26082144.

(46) Padavala, S. K. M.; Artyushkova, K.; Boettcher, S. W.; Nemšák, S.; Stoerzinger, K. A. Understanding Methanol Dissociative Adsorption and Oxidation on Amorphous Oxide Films. *Faraday Discuss.* **2022**, *236* (0), 58–70. https://doi.org/10.1039/D1FD00109D.
(47) Goyal, A.; Marcandalli, G.; Mints, V. A.; Koper, M. T. M. Competition between CO2 Reduction and Hydrogen Evolution on a Gold Electrode under Well-Defined Mass Transport Conditions. *J. Am. Chem. Soc.* **2020**, *142* (9), 4154–4161. https://doi.org/10.1021/jacs.9b10061.
(48) Bisht, A.; Zhang, P.; Shivakumara, C.; Sharma, S. Activity of Pt4+ Towards the CO Poisoning Effect in Formic Acid and Methanol Electro-Oxidation Compared to Pt Metal. *The Journal of Physical Chemistry* 34.
(49) Pala, R. G. S.; Tang, W.; Sushchikh, M. M.; Park, J.-N.; Forman, A. J.; Wu, G.; Kleiman-Shwarsctein, A.; Zhang, J.; McFarland, E. W.; Metiu, H. CO Oxidation by Ti- and Al-Doped ZnO: Oxygen Activation by Adsorption on the Dopant. *Journal of Catalysis* **2009**, *266* (1), 50–58. https://doi.org/10.1016/j.jcat.2009.05.011.